Mol Cell Biochem (2010) 344:117–124
DOI 10.1007/s11010-010-0535-1

Plasma membrane calcium ATPase isoform 3 expression in single cells isolated from rat liver

Blanca Delgado-Coello · Jorge Bravo-Martínez · Marcela Sosa-Garrocho · Marco A. Briones-Orta · Marina Macías-Silva · Jaime Mas-Oliva

Received: 17 December 2009 / Accepted: 23 June 2010 / Published online: 13 July 2010

Abstract The plasma membrane Ca^{2+}-ATPase (PMCA) located in the hepatocyte is a controversial molecule in itself since it displays different features to those regarded as canonical for P-type Ca^{2+}-ATPases, and from which transcript expression as well as catalytic activity continues to be under active investigation. Our aim in this study was to explore at a first glance, *pmca* isoform distribution using isolated parenchymal and non-parenchymal cells from rat liver tissue. Expression of *pmca* transcripts was analyzed in fresh or cell-enriched culture preparations, confirming *pmca1* and *pmca4* as the housekeeping isoforms in all cell types studied (hepatocytes, Kupffer cells, and stellate cells). However, for the first time we show expression of *pmca3* transcripts edited at two different sites in both hepatocytes and non-parenchymal cells. Interestingly, employing non-parenchymal cells we demonstrate the specific expression of *pmca3e* transcripts previously considered nearly exclusive of excitable tissues. Real-time PCR quantification shows a significant decrease of *pmca3* transcripts in cultured Kupffer and hepatic stellate cells in comparison with fresh cells. The presence of *pmca2* along with *pmca3* in all liver cell types studied suggests that high affinity isoforms are relevant to the adequate management of calcium in liver tissue, particularly when hepatic cells become activated by diverse stimuli.

Keywords Ca^{2+} homeostasis · Plasma membrane Ca^{2+}-ATPase · Hepatic parenchymal cells · Hepatic stellate cells · Kupffer cells · Single-cell RT-PCR

B. Delgado-Coello · M. Sosa-Garrocho · M. A. Briones-Orta · M. Macías-Silva · J. Mas-Oliva (✉)
Instituto de Fisiología Celular, Universidad Nacional Autónoma de México, Apartado Postal 70-243, 04510 Mexico, D.F., Mexico
e-mail: jmas@ifc.unam.mx

J. Bravo-Martínez
Facultad de Medicina, Universidad Nacional Autónoma de México, Apartado Postal 70-250, 04510 Mexico, D.F., Mexico

Present Address:
M. A. Briones-Orta
Cancer Research UK, London Research Institute, Lincoln's Inn Fields Laboratories, London, UK

Introduction

Metabolic homeostasis of the liver is maintained by the coordinated function performed by parenchymal (hepatocytes) and non-parenchymal cells. Non-parenchymal cells represent 20% of the hepatic mass and include Kupffer cells (KC), hepatic stellate cells (HSC), endothelial cells (EC), and lymphocytes. KC are resident macrophages that, in addition to performing phagocytosis of foreign molecules, produce cytokines as part of several immune responses [1]. HSC are devoted to the production of extracellular matrix and represent the most important site for storage of vitamin A in the organism. During liver regeneration, HSC and KC become activated, and begin to secrete growth modulators that are important in creating an optimal environment for recovery of the hepatic mass [2]. Activated KC showing evident morphologic changes are characterized by overproduction of inflammatory mediators and oxygen free radicals [3]. When HSC are activated in a chronic fashion, they play a relevant role in the process of liver fibrosis, exhibiting a myofibroblast-like phenotype in addition to overproduction of extracellular matrix proteins [4, 5].

A diversity of functions depends on calcium as a basic second messenger in signal transduction pathways modulating liver homeostasis. For instance, KC phagocytosis is Ca^{2+}-dependent, and the presence of specific membrane proteins mobilizing calcium such as L-type channels and store-operated Ca^{2+} channels has been described [6, 7]. Likewise, after liver injury HSC activation related to intracellular Ca^{2+} regulation has also been observed [8]. Contrary to what is observed in hepatocytes, quiescent and activated HSC present voltage-operated Ca^{2+} channels [9, 10].

As we have previously reviewed, the plasma membrane Ca^{2+}-ATPase (PMCA) seems to present a relevant function as a Ca^{2+} extrusion system in liver cells [11]. Four genes produce a large diversity of PMCA isoforms through a complex alternative splicing at two main sites: site A located near the phospholipid-sensitive domain, and site C located at the calmodulin (CaM)-binding domain of PMCA [12]. Although the presence in hepatic tissue of *pmca1* > *pmca4* > *pmca2* transcripts is well documented, much less knowledge is available considering *pmca* isoforms expression pattern in non-parenchymal cells [13, 14]. Expression of total PMCA in HSC caveolae and in EC fenestrae has been demonstrated by immunocytochemical methods [15, 16]. The presence of PMCA has been suggested in KC since a CaM-dependent Ca^{2+}-ATPase activity has been detected [17]. Nevertheless, specific PMCA isoforms expressed and their relevance in the phenomenon of activation in different liver cells remains unknown. Therefore, the aim of this study was to explore, as a first approach, *pmca* isoform transcript expression in isolated liver cells including hepatocytes, KC, and HSC immediately after isolation, as well as in primary cultures.

Materials and methods

Hepatocytes culture

Experimental animals were handled according to the Guide for the Care and Use of Laboratory Animals endorsed by the National Academy of Sciences (USA), in use in our Institute. Male Wistar rats weighing 250 g were anesthetized with an intramuscular injection of ketamine (40–80 mg/Kg) and xylazine (5–10 mg/Kg). Livers were perfused with a Krebs–Ringer solution (KR) containing 0.05% collagenase IV (Worthington, Lakewood, NJ, USA) [18]. Cell suspension was filtered and centrifuged at 500 rpm for 2 min; pellets were recovered and washed with KR to improve hepatocytes yielding.

For primary cultures, hepatocytes were resuspended in sterile PBS, diluted (v/v) with an isosmotic Percoll solution (45 mL Percoll/4.5 mL of 10× Hanks' balanced salt solution and 0.5 mL of 1 M Hepes) and centrifuged at 800 rpm for 5 min. Viabilities ≥85% were estimated by trypan blue exclusion. Hepatocytes were resuspended in Dulbecco's modified Eagle's medium (DMEM) plus 0.02% bovine serum albumin, 3 mM Hepes, 1 mM sodium piruvate, 6 mM sodium bicarbonate, 1 mg/mL galactose, 0.2 mM proline, 4 mM L-glutamine, 10% fetal bovine serum (FBS), 5 μg/mL insulin–transferrin–sodium-selenite (ITS), streptomycin (100 μg/mL), penicillin (100 U/mL), gentamicin (100 U/mL), and fungizone (0.25 μg/mL). Cells were plated in Petri dishes (2.5×10^6) and were allowed to attach during 3 h under a 5% CO_2/95% air atmosphere at 37°C. The medium was then replaced for serum-free DMEM with no added growth factors until cell collection was carried out after 2 days. The estimated viabilities did not change after this period of time.

Non-parenchymal cells culture

Male Wistar rats weighing 500 g were used for isolation of HSC and KC. Livers were perfused with KR and cells dissociated with 0.6–0.7% pronase and 0.15 μg/mL collagenase type IV according to a modified method by Tsukamoto et al. [19]. Digested tissue was minced, incubated with 20 μg/mL DNase I for 15 min at 37°C and separated in a Nycodenz gradient at 21,400 rpm for 45 min in a SW40 Ti rotor. HSC and KC were recovered from the 8.2 and 12% layers, respectively, and washed with PBS containing antibiotics and centrifuged at 2,500 rpm for 7 min. Cells were used immediately or placed in culture with a density of 3.5×10^6 in DMEM supplemented with 10% FBS plus antibiotics under a 5% CO_2/95% air atmosphere at 37°C. Culture medium was changed after 24 h and then every 2 days; the viabilities were as well ca. 85%.

Polymerase-chain-reaction methods

Total RNA was isolated from different cell types using the Trizol reagent and treated with Turbo DNase (Ambion, Inc., Austin, TX, USA). Oligonucleotides for rat *pmca* isoforms spliced at site C (Fig. 1) and rat and/or mouse glyceraldehyde-3-phosphate dehydrogenase (*GAPDH*) were designed with the MacVector 6.5.3 software, or as previously reported [20–24] (Table 1). One-step RT-PCRs were started with 0.5 μg of RNA in a final volume of 20 μL containing 0.25 μM of each primer (Invitrogen Carlsbad, CA, USA). Temperature steps were 50°C/30 min, 94°C/2 min for cDNA synthesis, followed by 40 cycles of the sequence 94°C/15 s, 55°C/30 s, 72°C/1 min, and a 10-min extension step. Markers for HSC and EC were amplified using 25 cycles [22, 23]. PCR products were separated in 4% ethidium bromide-stained agarose gels.

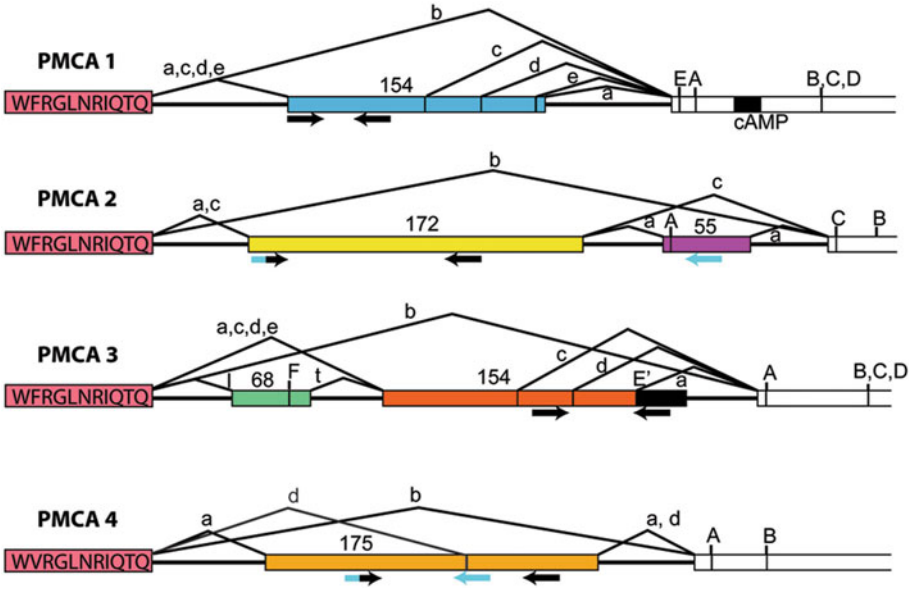

Fig. 1 Primer design used for amplification of rat *pmca* transcripts spliced at site C. Conserved sequences codifying the constant region of CaM-binding domain are indicated (*pink boxes*) (24). Primers for *pmca1* recognize isoform "1c" (66 bp). Primers for *pmca3* align in the 154 bp exon (number 23) and in an extension of exon 23 (*black box*) producing variant "3e" (82 bp) [24, 31]. For *pmca2* and *pmca4* two primer pairs were designed; forward primers were common to two alternative isoforms (*blue/black arrows*). Primers for *pmca2* recognize sites in the 172-bp exon of variant "2c" (132 bp) or variant "2a" (199 bp) including both exons. Primers for *pmca4* amplify two different fragments of variant "4a" (115 and 77 bp, respectively). (Color figure online)

Table 1 Primers employed for RT-PCR analysis

Gene	Forward (5′–3′)	Reverse (5′–3′)	Size (bp)
pmca1 [20]	GGCGACTTTGGCATCACACT	TTTCAACTTGGTGCAAATTCCA	120
pmca2 [21]	AAGGAGACATATGGGGAC	TTCACCTTCATCTTCTGC	300
pmca3 [21]	CACAGCCTTCAATGACTG	CCTTCCATGACATGAGTG	300
pmca1c	GGATGTAGTGAATGCTTTCCAG	ATGGAGGGTTGTCGCCTTAG	66
pmca2c	CAATACTTTCAAGAGCGGG	GGAGAGGAAAGAGCATTGGATAAC	132
pmca2a	CAATACTTTCAAGAGCGGG	TCTCTTGCTGAACTCTGTGTC	199
pmca3e	GTAACCAATCTTTCTACCCC	TTTCACCACTCGGATTGC	82
pmca4a	AGTCCTAAGGCGACAGAACTTGAG	TGTAACGGCAGAAGAGGTGGAG	115
pmca4a′	AGTCCTAAGGCGACAGAACTTGAG	ACGCAACTGCTTCTGAATAG	77
PPARγ [22]	ATTCTGGCCCACCAACTTCGG	TGGAAGCCTGATGCTTTATCCCCA	332
α-SMA [22]	TGTGCTGGACTCTGGAGATG	GATCACCTGCCCATCAGG	292
ELAM1 [23]	CAACGTGCACGTTTGACTGT	AGGTCAAGGCTTGAACACTG	508
m/rGAPDH	GGAGAAACCTGCCAAGTATGATGAC	TGGGAGTTGCTGTTGAAGTCG	126
rGAPDH	TCCCAGAGCTGAACGGGAAG	TTACTCCTTGGAGGCCATGTAG	325

NCBI accession numbers: *pmca1*, NM_053311; *pmca2*, NM_012508; *pmca3*, NM_133288; *pmca4*, NM_001005871

Single-cell RT-PCR

Single hepatocytes as well as KC and HSC were harvested under a differential interference contrast (DIC) infrared microscope (Nikon FN1) from <24-h cultures employing a whole-cell configuration and recovered applying negative pressure into the glass pipette. Each single cell was collected in sterile tubes containing RNAse inhibitors, frozen in liquid nitrogen and kept at −70°C until use. Isolated hepatocytes were treated with DNase I and used immediately for RT-PCR with the AccessQuick™ system (Promega Co., Madison, WI, USA) using 50 cycles for amplification as reported by us [25]. PCR products were separated in 3% agarose-TBE gels, soaked in SYBR Safe stain (Invitrogen, Carlsbad, CA, USA) for 1 h, and analyzed in a Typhoon 9400 scanner (GE Healthcare).

Real-time RT-PCR

Specific primers for *pmca3* (NM_133288), forward 5′-GCAGATGTTGTGGGTGAACT-3′, reverse 5′-CGTG AGATGAGAGGCTTGTC-3′, and the Taqman probe CTT CCGCA GCAGCAGTGACTCAGTTG were designed (Primer Design Ltd, Southampton, UK). One-step quantitative-PCR assays using total RNA (0.5 μg) from fresh and cultured hepatocytes, KC and HSC were performed according to the following program: 50°C/15 min, 95°C/2 min and 40 cycles at 95°C/15 s, 60°C/40 s in an ABI Prism 7000 detection system from Applied Biosystems (Foster City, CA, USA).

Results

pmca transcripts in hepatocytes

pmca1 and *pmca4* isoforms are abundantly expressed in fresh hepatocytes (Fig. 2a) and those maintained for 2 days in culture (data not shown). Since the use of end-point PCR techniques did not allow us to discriminate differences in the expression pattern between fresh and 2-day hepatocytes, we only show results using fresh cells. In general terms, *pmca2* transcripts edited upstream of site A (UA) and exhibit a higher level of expression than those spliced at site C. We consistently found the expected *pmca3* isoform (UA, 300 bp) and a second band (~650 bp) identified as a member of the toll-like receptor family (TLR3), which has been found in hepatocytes and KC [26, 27]. Products obtained with primers designed for *pmca2a* and *pmca3e* (site C) showed low concentration bands that did not correspond to the expected size, therefore they were not included in the corresponding figure (Fig. 2a).

In addition, we show in hepatocytes the presence of the *peroxisome proliferator-activated receptor γ* (*PPARγ*) and *α-smooth muscle actin* (*α-SMA*) transcripts described as markers and whose expression specifically diminishes or becomes induced in activated HSC [22]. In contrast, the marker for EC, *E-Selectin* (*ELAM-1*) [23] was absent (Fig. 2a). Since some contamination from non-parenchymal cells during hepatocyte isolation is feasible, we decided to collect single hepatocytes (Fig. 2b) and confirmed the presence of *pmca3* (UA) and *PPARγ* transcripts using a system detecting targets at the zeptomolar level (Fig. 2c). In our hands, employing isolated hepatocytes it was not possible to amplify transcripts <200 bp including rat/mouse *GAPDH* (126 bp); therefore, rat *GAPDH* primers yielding 325-bp amplicons were used (Table 1).

Using real-time PCR as the most sensitive technique available, the *pmca3* isoform (site C) was quantified in fresh and cultured hepatocytes showing no apparent differences (Fig. 2d).

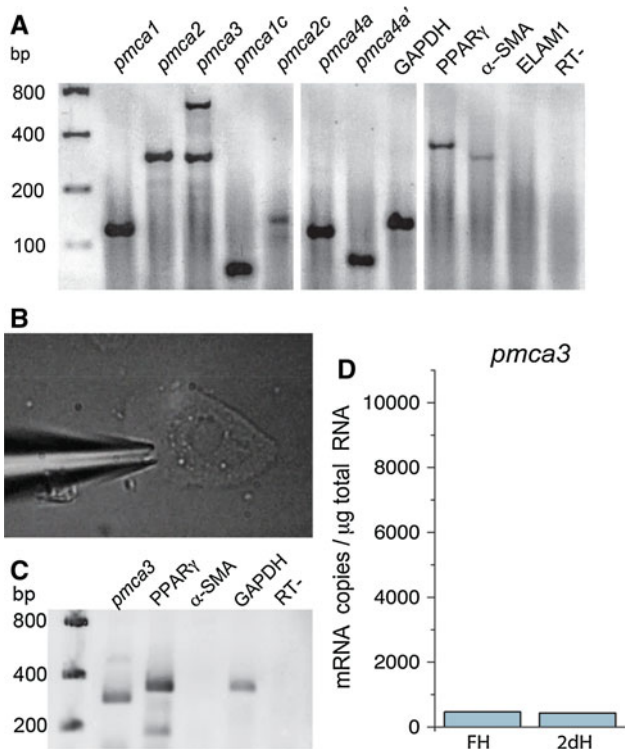

Fig. 2 Analysis of *pmca* transcripts expressed in hepatocytes. **a** Representative experiment showing *pmca* transcripts of edited upstream of site A (*pmca1-3*), and site C from fresh hepatocytes-enriched preparations (*FH*). **b** Single hepatocyte harvested under a DIC infrared microscope in a whole-cell configuration. **c** Sybr Safe-stained gel showing transcripts from single independent hepatocytes, confirming expression of *pmca3* and *PPARγ*. **d** Representative experiment (from three experiments) using triplicates showing real-time PCR quantification of *pmca3* transcripts (site C) in *FH* and hepatocytes placed 2 days in culture (*2dH*). Mean values ± SE in FH (470.37 ± 0.85) and in 2dH (429 ± 0.83). The *y* axis scale is the same as in Figs. 3d and 4d

pmca transcripts in Kupffer cells (KC)

In KC, the most abundant *pmca* transcripts show to be the housekeeping isoforms *pmca1* and *pmca4* spliced in both explored sites, followed by the *pmca2* and *pmca3* isoforms (UA, Fig. 3a). *TLR3* transcripts were also detected in amplifications with primers for *pmca3* (UA). A slight ~199-bp band corresponding to *pmca2a* transcripts was visualized in addition to several unspecific transcripts. Interestingly, *pmca3e* was detected under all conditions and its identity was determined by automated sequencing. Transcripts corresponding to *PPARγ*, *α-SMA* and to a lesser extent *ELAM-1* were evident in KC fractions. The presence of *pmca3e* transcripts was confirmed in single KC (Fig. 3c).

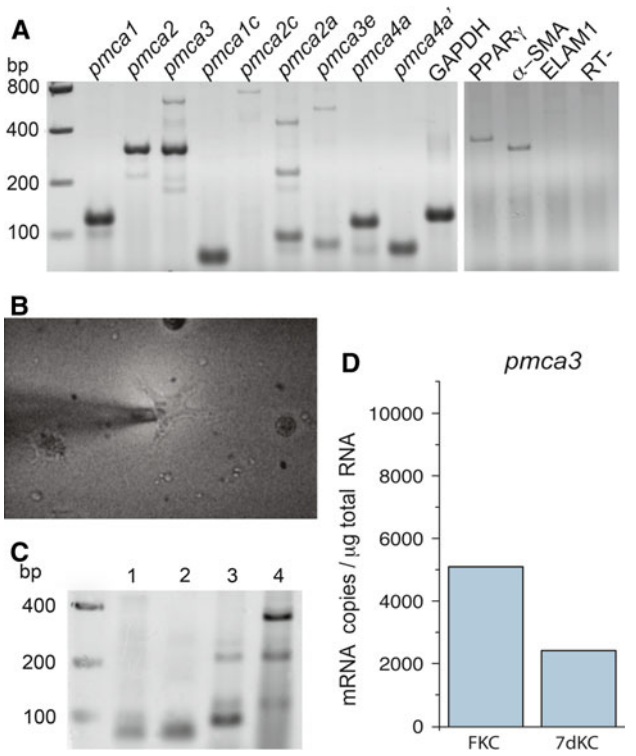

Fig. 3 Analysis of *pmca* transcripts expressed in Kupffer cells. **a** Representative experiment showing *pmca* transcripts edited upstream of site A (*pmca1-3*), site C, together with activation markers from fresh KC-enriched (FKC) preparations. **b** Single KC harvested under a DIC infrared microscope in a whole-cell configuration. **c** Sybr Safe-stained gel showing *pmca3e* transcripts (82 bp) expressed in a single fresh KC (*lane 1*); in 10 isolated KC (*lane 2*); in fresh KC-enriched preparations (*lane 3*) and KC after 7 days in culture (7 days KC, *lane 4*). **d** Representative experiment (from three experiments) using triplicates showing real-time PCR quantification of *pmca3* transcripts (site C). Mean values ± SE in FKC (5,116.78 ± 1.19) and in 7 days KC (2,439.78 ± 0.80). The *y* axis scale is the same as in Figs. 2d and 4d

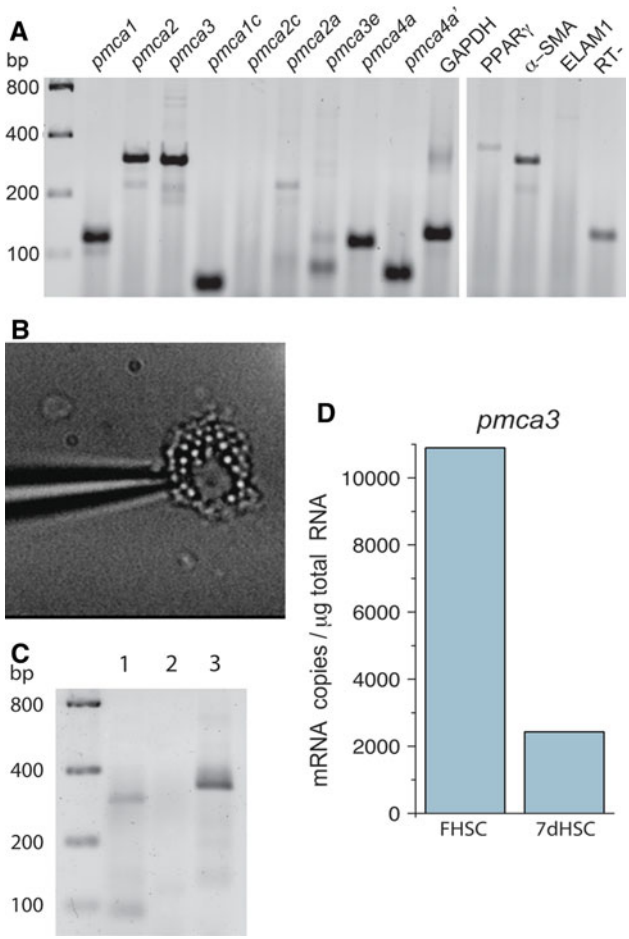

Fig. 4 Analysis of *pmca* transcripts expressed in hepatic stellate cells (HSC). **a** Representative experiment showing *pmca* transcripts edited upstream of site A (*pmca1-3*), site C together with activation markers from fresh HSC. **b** Single-HSC harvested under a DIC infrared microscope in a whole-cell configuration, showing the typical vitamin A droplets associated to this cell type. **c** Sybr Safe-stained gel showing transcripts using total RNA (200 ng) from fresh HSC; *lane 1*, *pmca3* edited upstream site A (300 bp); *lane 2*, *pmca3e* (site C), non-detected; *lane 3*, *GAPDH* (325 bp). **d** Representative experiment (from three experiments) using triplicates showing real-time PCR quantification of *pmca3* transcripts (site C). Mean values ± SE in FKC (5,116.78 ± 1.19) and in 7 days KC (2,439.78 ± 0.80). The *y* axis scale is the same as in Figs. 2d and 3d

Since we observed apparent changes in expression of *pmca3e* in KC cultured for 7 days (Fig. 3c), we further explored *pmca3* using real-time PCR techniques. In experiments with total RNA obtained from KC-enriched preparations, after 7 days in culture we observed a lower level of *pmca3* expression (Fig. 3d).

pmca transcripts in hepatic stellate cells (HSC)

In HSC, a similar expression pattern to that of hepatocytes and KC for *pmca1* and *pmca4* isoforms can be observed (Fig. 4). In addition, the expected amplicon for *pmca3* (UA) was observed with a higher level of expression, in contrast to that spliced at site C. In a similar fashion to that observed in KC, *pmca2c* (132 bp) is absent, while *pmca2a* (~199 bp) is slightly expressed (Table 2). *PPARγ* and *α-SMA* transcripts were always observed in fresh HSC, while *ELAM-1* transcripts were absent (Fig. 4). At the

Table 2 Summary of *pmca* transcripts expressed in different cell types contained in the liver

Cell type	Site UA			Site C					
	1	*2*	*3*	*1c*	*2c*	*2a*	*3e*	*4a*	*4a'*
Hepatocytes	++	++	++	++	+	−	−	++	++
Kupffer cells	++	++	++	+	−	+	+	++	++
Stellate cells	++	++	++	++	−	+	+	++	++

++ high level of expression, + moderate expression, + low level of expression, − absent or showing a different size

single-cell level, *pmca3e* transcripts were out of the detection limits of our amplification system (AccessQuick™), and therefore only found in experiments using 100–200 ng of RNA isolated from several HSC (Fig. 4c). However, the detection of *pmca3* (site C) transcripts was accomplished in single-HSC using real-time PCR with an expression of ≤10 mRNA copies/cell. Further experiments using real-time PCR and total RNA isolated from HSC, showed a diminished level of expression of *pmca3* in cells maintained in culture for 7 days (Fig. 4d).

Discussion

To date, relevant proteins involved in Ca^{2+} homeostasis at the intracellular and extracellular levels together with the expression of a G-protein-coupled receptor that senses extracellular Ca^{2+} levels in the hepatocyte are well known [28, 29]. Nevertheless, the participation of the several Ca^{2+} extrusion systems described in liver cells such as the PMCA and the NCX are less understood [11]. For the first time, our study explores *pmca* isoform expression in liver using freshly isolated and cultured hepatocytes, KC- and HSC-enriched preparations. Analysis of *pmca* transcript expression in human and rat liver show the presence of *pmca1*, followed by *pmca4*, and *pmca2* [13, 14]. However, the presence of *pmca3* transcripts has not been demonstrated in liver yet, probably due to the use of degenerate primers and the complex splicing pattern displayed by *pmca* encoding genes [30]. The important expression of *pmca3* transcripts (UA) and the moderate expression of *pmca3* (site C) in all liver cell types studied was confirmed at the single-cell level using either a sensitive end-point PCR kit (AccessQuick™) or through real-time PCR.

Interestingly, *pmca3e* transcripts were only observed in non-parenchymal cells (Figs. 3, 4; Table 2). The 3′ end of these transcripts aligns to a sequence located in an 88-bp extension of the 154-bp exon (exon 23) included in exon 24 (Fig. 1), which is expressed in rat skeletal muscle as well as in brain mRNAs [31]. In the human, this variant is present in fetal skeletal muscle [13] and the complete sequence of *pmca3* is also reported in brain [32]. Exon 24 can be translated according to two reading frames depending upon the upstream splice site, followed by an alternative polyA signal. The presence of acidic (A) or basic (B) CaM-binding domains in the PMCA expressed possesses important physiological implications, such as the type B CaM-binding site which displays a significantly higher affinity for CaM (up to 10-fold) and a higher autoinhibitory capacity (15-fold) than the type A CaM-binding site [33]. Since the CaM-binding site encoded by exon 24 corresponds to a B form, the physiological relevance for the presence of these *pmca3* transcripts in non-parenchymal cells is open to investigation.

It is noticeable that real-time PCR using primers detecting *pmca3* (site C) were able to detect transcripts in different RNA preparations from hepatocytes that in comparison to non-parenchymal cells were less abundant (Fig. 2d). Moreover, this isoform seems to be non-relevant when studied in fresh or 2-day cultured hepatocytes. This might reflect the fact that under these conditions cells never have been under the effect of added growth factors that trigger replication in vitro and dedifferentiation normally observed in long-term cultured hepatocytes.

Data from real-time PCR show a 50% decrease in the level of expression observed for *pmca3* in KC cultured for 7 days in comparison to fresh KC (Fig. 3d). Although primary cultures of KC are not considered to be involved in a possible activation process by itself, based on published evidence we believe this might be the case. Since it has been recognized that non-parenchymal cells might become activated during the cell's isolation procedure [34], we believe this phenomenon is occurring with our KC placed in culture. Taking into consideration that KC become activated after CCl_4-treatment or as a result of exposition to bacterial extracts showing an important induction of osteopontin mRNA expression [35, 36], we searched for osteopontin transcripts in our KC preparations. We found that osteopontin is expressed in both fresh and cultured KC suggesting that the process of activation is taking place after KC isolation (data not shown). Since our group has recently correlated the overexpression of osteopontin with the process of atherosclerosis through the induction of a state of oxidative stress (Jiménez-Corona et al., submitted), this phenomenon might be related to the activation of our KC and therefore it will be further studied.

On the other hand, one interesting although controversial hypothesis suggests a neuroendocrine origin for HSC based on the fact these cells share the expression of several markers observed in nervous system cells [37–39]. The presence of *pmca3e* transcripts in HSC seems to reinforce this notion, since the possibility that nerve endings might be contaminating HSC preparations [40] was discarded with the use of single-HSC experiments (Fig. 4b) where *pmca3* (site C) was quantitatively measured.

Since PMCA3 and PMCA2 are considered isoforms that show the highest affinities for Ca^{2+} and CaM reported among the four PMCA isoforms, it will be interesting to elucidate in non-parenchymal hepatic cells the function associated to these "fast" isoforms (mainly present in excitable tissues). For several PMCA2 isoforms spliced at site A and for PMCA3a in the presence of CaM, apparent K_m Ca^{2+} constants range between 0.3–0.5 μM and K_m CaM up to 10 nM [41, 42]. The highest affinities comprise those from PMCA2 variants spliced at site C, 2a

(K_m Ca^{2+} 0.09 μM/K_m CaM 8.4 nM), and 2b (K_m Ca^{2+} 0.06 μM/K_m CaM 2.1 nM) [43]. In contrast, Ca^{2+} affinity for PMCA4b is ca. 0.5 μM, and CaM affinity ca. 50–100 nM [41]. These contrasting kinetic properties are closely related with the ability of individual PMCAs to restore the intracellular calcium concentration after an inward movement of calcium has occurred [44]. Since non-parenchymal cells play a relevant role in supporting hepatocyte survival after diverse stimuli, efficient PMCA isoforms must be readily available to maintain Ca^{2+} homeostasis in the whole organ. In this respect, it is important to note that activated HSC showing contractile activity [45, 46] must also require the presence of PMCAs to modulate the intracellular levels of calcium and therefore their contractile function.

In order to understand the genotype changes that seem to affect different liver cells or the way in which the post-activation process could be interpreted, a temporal course of changes after seeding cells in culture must be analyzed. Also, the complete analysis of expression changes occurring with other *pmca* variants that could counteract the specific decrease of *pmca3* transcripts detected in cultured KC will be carried out. The present study in the near future will help us to solve many of the questions still unanswered related to the function of the dynamic changes in the levels and isoform type of the plasma membrane calcium pump in non-excitable cells.

Acknowledgments The authors thank Angel Zarain-Herzberg for advice on the design of oligonucleotides and members of the Molecular Biology Unit at IFC for their technical support. We also thank Paul Gaytán, Santiago Becerra, Jorge Yañez and Eugenio López for synthesis of oligonucleotides and DNA sequencing, and Héctor Malagón for excellent care of experimental animals. This work was partially supported by CONACyT (Grant 47333/A-1) and DGAPA-UNAM (Grant IN228607/19) awarded to J. M–O.

References

1. Taub R (2004) Liver regeneration: from myth to mechanism. Nat Rev Mol Cell Biol 5:836–847
2. Santoni-Rugiu E, Jelnes P, Thorgeirsson SS, Bisgaard HC (2005) Progenitor cells in liver regeneration: molecular responses controlling their activation and expansion. APMIS 113:876–902
3. Hijioka T, Rosenberg RL, Lemasters JJ, Thurman RG (1992) Kupffer cells contain voltage-dependent calcium channels. Mol Pharmacol 41:435–440
4. Friedman SL, Wei S, Blaner WS (1993) Retinol release by activated rat hepatic lipocytes: regulation by Kupffer cell-conditioned medium and PDGF. Am J Physiol 264:G947–G952
5. Ballardini G, Fallani M, Biagini G et al (1988) Desmin and actin in the identification of Ito cells and in monitoring their evolution to myofibroblasts in experimental liver fibrosis. Virchows Arch B Cell Pathol Incl Mol Pathol 56:45–49
6. Yamada S, Mochida S, Ohno A et al (1991) Evidence for enhanced secretory function of hepatic macrophages after long-term ethanol feeding in rats. Liver 11:220–224
7. Jiang N, Zhang ZM, Liu L et al (2006) Effects of Ca^{2+} channel blockers on store-operated Ca^{2+} channel currents of Kupffer cells after hepatic ischemia/reperfusion injury in rats. World J Gastroenterol 12:4694–4698
8. Murata T, Aria S, Mori A, Imamura M (2003) Therapeutic significance of Y-27632, a Rho-kinase inhibitor, on the established liver fibrosis. J Surg Res 114:64–71
9. Oide H, Thurman RG (1994) Hepatic Ito cells contain calcium channels: increases with transforming growth factor-beta 1. Hepatology 20:1009–1014
10. Oide H, Tateyama M, Wang XE et al (1999) Activated stellate (Ito) cells possess voltage-activated calcium current. Biochim Biophys Acta 1418:158–164
11. Delgado-Coello B, Trejo R, Mas-Oliva J (2006) Is there a specific role for the plasma membrane Ca^{2+}-ATPase in the hepatocyte? Mol Cell Biochem 285:1–15
12. Strehler EE, Zacharias DA (2001) Role of alternative splicing in generating isoform diversity among plasma membrane calcium pumps. Physiol Rev 81:21–50
13. Stauffer TP, Hilfiker H, Carafoli E, Strehler EE (1993) Quantitative analysis of alternative splicing options of human plasma membrane calcium pump genes. J Biol Chem 268:25993–26003
14. Delgado-Coello B, Santiago-García J, Zarain-Herzberg A, Mas-Oliva J (2003) Plasma membrane Ca^{2+}-ATPase mRNA expression in murine hepatocarcinoma and regenerating liver cells. Mol Cell Biochem 247:177–184
15. Ogi M, Yokomori H, Inao M, Oda M, Ishii H (2000) Hepatic stellate cells express Ca^{2+} pump-ATPase and Ca^{2+}-Mg^{2+}-ATPase in plasma membrane caveolae. J Gastroenterol 35:912–918
16. Yokomori H, Oda M, Ogi M et al (2000) Hepatic sinusoidal endothelial fenestrae express plasma membrane Ca++ pump and Ca++Mg++-ATPase. Liver 20:458–464
17. Birmelin M, Marme D, Ferber E, Decker K (1984) Calmodulin content and activity of Ca^{2+}-ATPase and phospholipase A2 in rat Kupffer cells. Eur J Biochem 40:55–61
18. Berry MN, Friend DS (1969) High-yield preparation of isolated rat liver parenchymal cells: a biochemical and fine structural study. J Cell Biol 43:506–520
19. Tsukamoto H, Cheng S, Blaner WS (1996) Effects of dietary polyunsaturated fat on ethanol-induced Ito cell activation. Am J Physiol 270:G581–G586
20. Mamic TM, Holman NA, Roberts-Thomson SJ, Monteith GR (2000) PMCA1 mRNA expression in rat aortic myocytes: a real time RT-PCR study. Biochem Biophys Res Commun 276:1024–1027
21. Souza KL, Elsner M, Mathias PC, Lenzen S, Tiedge M (2004) Cytokines activate genes of the endocytotic pathway in insulin-producing RINm5F cells. Diabetologia 47:1292–1302
22. Miyahara T, Schrum L, Rippe R et al (2000) Peroxisome proliferator-activated receptors and hepatic stellate cell activation. J Biol Chem 275:35715–35722
23. Wang X, Yue TL, Barone FC, Feuerstein GZ (1995) Demonstration of increased endothelial-leukocyte adhesion molecule-1 mRNA expression in rat ischemic cortex. Stroke 26:1665–1669
24. Keeton TP, Burk SE, Shull GE (1993) Alternative splicing of exons encoding the calmodulin-binding domains and C termini of plasma membrane Ca^{2+}-ATPase isoforms, 1, 2, 3, and 4. J Biol Chem 268:2740–2748
25. Delgado-Coello B, Bravo-Martínez J, Mas-Oliva J (2009) Detecting PMCA transcripts in single hippocampal neurons. http://www.promega.com/pubs/tub_010.htm
26. Wu J, Lu M, Meng Z et al (2007) Toll-like receptor-mediated control of HBV replication by non parenchymal liver cells in mice. Hepatology 46:1769–1778
27. Isogawa M, Robek MD, Furuichi Y, Chisari FV (2005) Toll-like receptor signaling inhibits hepatitis B virus replication in vivo. J Virol 79:7269–7272

28. Barritt GJ, Chen J, Rychkov GY (2008) Ca^{2+} permeable channels in the hepatocyte plasma membrane and their roles in hepatocytes physiology. Biochim Biophys Acta 1783:651–672
29. Canaff L, Petit J-L, Kisiel M et al (2001) Extracellular calcium-sensing receptor is expressed in rat hepatocytes. J Biol Chem 276:4070–4079
30. Howard A, Barley NF, Legon S, Walters JRF (1994) Plasma-membrane calcium-pump isoforms in human and rat liver. Biochem J 303:275–279
31. Burk SE, Shull GE (1992) Structure of the rat plasma membrane Ca^{2+}-ATPase isoform 3 gene and characterization of alternative splicing and transcription products. J Biol Chem 267:19683–19690
32. Brown BJ, Hilfiker H, DeMarco SJ et al (1996) Primary structure of human plasma membrane Ca^{2+}-ATPase isoforms 3. Biochim Biophys Acta 1283:10–13
33. Enyedi A, Filoteo AG, Gardos G, Penniston JT (1991) Calmodulin-binding domains from isozymes of the plasma membrane Ca^{2+} pump have different regulatory properties. J Biol Chem 266:8952–8956
34. Malik R, Selden C, Hodgson H (2002) The role of non-parenchymal cells in liver growth. Semin Cell Dev Biol 3:425–431
35. Kawashima R, Mochida S, Matsui A et al (1999) Expression of osteopontin in Kupffer cells and hepatic macrophages and stellate cells in rat liver after carbon tetrachloride intoxication: a possible factor for macrophage migration into hepatic necrotic areas. Biochem Biophys Res Commun 256:527–531
36. Wang Y, Mochida S, Kawashima R et al (2000) Increased expression of osteopontin in activated Kupffer cells and hepatic macrophages during macrophage migration in Propionibacterium acnes-treated rat liver. J Gastroenterol 35:696–701
37. Friedman SL (2008) Hepatic stellate cells: protean, multifunctional, and enigmatic cells of the liver. Physiol Rev 88:125–172
38. Sato M, Suzuki S, Senoo H (2003) Hepatic stellate cells: unique characteristics in cell biology and phenotype. Cell Struct Funct 28:105–112
39. Asahina K, Tsai SY, Li P et al (2009) Mesenchymal origin of hepatic stellate cells, submesothelial cells, and perivascular mesenchymal cells during mouse liver development. Hepatology 49:998–1011
40. Bioulac-Sage P, Lafon ME, Saric J, Balabaud C (1990) Nerves and perisinusoidal cells in human liver. J Hepatol 10:105–112
41. Hilfiker H, Guerini D, Carafoli E (1994) Cloning and expression of isoform 2 of the human plasma membrane Ca^{2+} ATPase. Functional properties of the enzyme and its splicing products. J Biol Chem 269:26178–26183
42. Brini M, Coletto L, Pierobon N et al (2003) A comparative functional analysis of plasma membrane Ca^{2+} pump isoforms in intact cells. J Biol Chem 278:24500–24508
43. Elwess NL, Filoteo AG, Enyedi A, Penniston JT (1997) Plasma membrane Ca^{2+} pump isoforms 2a and 2b are unusually responsive to calmodulin and Ca^{2+}. J Biol Chem 272:17981–17986
44. Strehler EE, Caride AJ, Filoteo AG et al (2007) Plasma membrane Ca^{2+} ATPases as dynamic regulators of cellular calcium handling. Ann NY Acad Sci 1099:226–236
45. Kawada N, Klein H, Decker K (1992) Eicosanoid-mediated contractility of hepatic stellate cells. Biochem J 285:367–371
46. Sakamoto M, Ueno T, Kin M et al (1993) Ito cell contraction in response to endothelin-1 and substance P. Hepatology 18:978–983